Observation of Infinite-Range Intensity Correlations above, at, and below the Mobility Edges of the 3D Anderson Localization Transition

W. K. Hildebrand,[1] A. Strybulevych,[1] S. E. Skipetrov,[2] B. A. van Tiggelen,[2] and J. H. Page[1,*]
[1]Department of Physics and Astronomy, University of Manitoba, Winnipeg, Manitoba, Canada R3T 2N2
[2]Université Grenoble 1/CNRS, LPMMC UMR 5493, B.P. 166, 38042 Grenoble, France
(Received 26 March 2013; published 19 February 2014)

We investigate long-range intensity correlations on both sides of the Anderson transition of classical waves in a three-dimensional disordered material. Our ultrasonic experiments are designed to unambiguously detect a recently predicted infinite-range C_0 contribution, due to local density of states fluctuations near the source. We find that these C_0 correlations, in addition to C_2 and C_3 contributions, are significantly enhanced near mobility edges. Separate measurements of the inverse participation ratio reveal a link between C_0 and the anomalous dimension Δ_2, implying that C_0 may also be used to explore the critical regime of the Anderson transition.

DOI: 10.1103/PhysRevLett.112.073902 PACS numbers: 42.25.Dd, 43.20.Gp, 64.60.al, 71.23.An

The phenomenon of Anderson localization—the halt of wave transport due to destructive interferences of scattered waves—was first discovered for electrons in disordered solids [1–6]. John [7,8] and Anderson [9] later suggested that it may also take place for classical waves, such as sound or light. The latter open up new ways to study Anderson localization that would be difficult, or even impossible, to implement in electronic systems. Time- and position-resolved measurements, for example, have enabled the first unambiguous observation of three-dimensional (3D) Anderson localization of elastic waves [10] and yield promising results for light [11]. Further insight into this unique regime of wave physics can be gained by investigating the correlations of the intensity fluctuations that constitute speckle patterns. While short- and long-range correlations of the intensity (denoted C_1, C_2, C_3) [12–19], and even phase [20,21], have been predicted and observed in the regime of weak disorder, they remain unexplored in the localized regime and at the mobility edge (ME) where the transition between diffuse and localized behavior occurs. Moreover, a new type of infinite-range intensity correlation (denoted C_0), originating from scattering in the vicinity of the source, has recently been predicted [22,23]. For a point source embedded in a disordered medium, this correlation was shown to be closely related to fluctuations of the local density of states (LDOS) at the source position [24,25]. Hence, providing that an appropriate source type is used [26], the recent measurements of LDOS fluctuations [27–30] can be considered as indirect evidence for infinite-range C_0 correlations. LDOS fluctuations are expected to grow as the states become spatially localized [28,30,31], with recent theoretical studies even reporting their variance to behave as a one-parameter scaling function of sample size and localization length [32,33]; this means they constitute a new tool to provide insight into the Anderson transition. In view of the profusion of results concerning LDOS fluctuations, it is remarkable that no direct measurement of the C_0 contribution to the intensity correlation function has been reported so far [34].

In this Letter, we present the first direct experimental evidence of infinite-range (C_0) spatial and frequency correlations of intensity above, at, and below the ME of the Anderson transition of a disordered, strongly scattering 3D material. The experiments were performed using ultrasonic techniques on samples in which 3D Anderson localization of ultrasound has been demonstrated previously [10]. Comparison of experiment with theory, coupled with complementary measurements designed to suppress infinite-range correlations when desired, allows the C_0 contribution to the correlations to be clearly separated from the other contributions (C_1, C_2, or C_3), unambiguously revealing the presence of large infinite-range correlations. We observe that these correlations grow dramatically near the ME in our samples. Motivated by the prediction that the LDOS fluctuations are closely related to multifractality of the wave functions through the $q = 2$ generalized inverse participation ratio [28,33], we measure the anomalous dimension Δ_2 for our samples in independent experiments and find good correspondence between this quantity and measured C_0 correlations. This clearly demonstrates the link between multifractality, C_0, and the LDOS fluctuations.

The samples investigated are disordered elastic networks of aluminum beads, weakly brazed together to form slabs (see Supplemental Material [35]). This porous mesoscale structure leads to very strong scattering with low absorption in the frequency range investigated (~0.5–2.5 MHz), a crucial feature for the observation of 3D Anderson localization of ultrasound in this material. The mesoscale structure also leads to high contrast in the density of states of the aluminum matrix compared to that of the pores—yet

another reason for anticipating strong fluctuations of the LDOS. The samples were waterproofed so that the experiments could be performed in a water tank with either vacuum or air in the pores, thereby ensuring that the detected transmitted waves had traveled only through the aluminum bead network.

In our experiments, a tightly focused broadband ultrasonic pulse (with beam waist smaller than the wavelength) is incident on the sample, and the transmitted pressure is detected in the near field by a subwavelength hydrophone [35]. To capture contributions to C_0 due to LDOS fluctuations at both the focal point of the incident wave (source point) and the detector, we scan both the source and detector over the surface of the sample. The recorded pressure fields $p(\mathbf{r}, t)$ are Fourier transformed to obtain the intensity $I(\mathbf{r}, \omega) \propto |p(\mathbf{r}, \omega)|^2$ as a function of frequency for each pair of source and detector positions. The intensity correlation function is calculated as

$$C_\omega(\Delta r, \Omega) = \frac{\langle \delta I(\mathbf{r}, \omega - \frac{1}{2}\Omega) \delta I(\mathbf{r} + \Delta\mathbf{r}, \omega + \frac{1}{2}\Omega) \rangle}{\langle I(\mathbf{r}, \omega - \frac{1}{2}\Omega) \rangle \langle I(\mathbf{r} + \Delta\mathbf{r}, \omega + \frac{1}{2}\Omega) \rangle}, \quad (1)$$

where the angular brackets denote ensemble averaging and $\delta I = I - \langle I \rangle$ is the fluctuation of the intensity. Ensemble averaging is done by scanning over many source and detector positions corresponding to the same Δr. For comparison, experiments with a single (stationary) source point were also performed, in which case the ensemble averaging was done only over all possible detector positions; this suppresses C_0 correlations due to LDOS fluctuations at the source. In what follows we will study spatial correlations $C_\omega(\Delta r) = C_\omega(\Delta r, 0)$ and frequency correlations $C_\omega(\Omega) = C_\omega(0, \Omega)$ separately.

Figure 1 shows the spatial correlations measured near $f = \omega/2\pi = 2.4$ MHz, the frequency at which Anderson localization of elastic waves was demonstrated in this sample [10]. For both types of experiments, the correlations decay rapidly at small Δr due to C_1, with a slower decay due to C_2 and C_3 that extends out to $\Delta r \sim 10$ mm, beyond which $C_\omega(\Delta r)$ becomes independent of distance. For the data where the source position is varied, an asymptotic value of order unity is seen for the correlations, showing clear evidence of a C_0 term due to LDOS fluctuations at the source. By contrast, no infinite-range correlations are seen for the single-source data, consistent with the fact that the LDOS at the source position does not fluctuate in this case.

To gain further insight into this behavior, we compare our experimental data with theoretical calculations. We compute C_1, C_2, C_3, and C_0 correlation functions assuming weak disorder ($k\ell \gg 1$, where k is the wave number in the medium and ℓ is the mean free path) and write the full correlation $C_\omega(\Delta r)$ as a function of three fit parameters: A, $C_0^{(\mathrm{in})}$, and $C_0^{(\mathrm{out})}$. Although this calculation is not exact, the parametrization into four fundamentally different classes of speckle correlations involving phenomenological constants

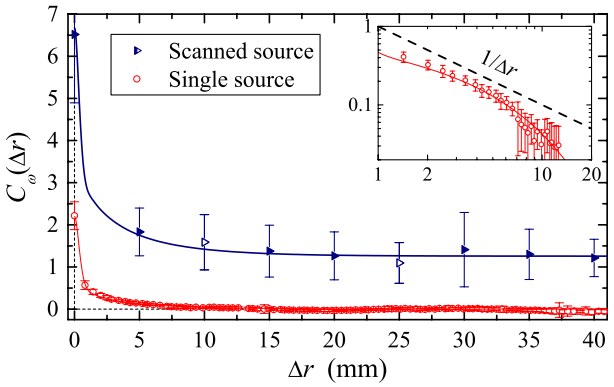

FIG. 1 (color online). Spatial intensity correlations for the two types of experiments at 2.4 MHz. The scanned-source data show convincing evidence of infinite-range (C_0) correlations, which are suppressed when only a single source point is used. Lines are theoretical fits using the values of parameters given in Table I. The inset shows the single-source data on a log-log scale in order to reveal the extent to which the expected $1/\Delta r$ dependence is observed for C_2 and C_3 at intermediate length scales. Data have been averaged over a bandwidth of 750 kHz, and the error bars are the standard deviations associated with the data's statistical fluctuations, which are observed to be inherently large near the Anderson transition. (The open symbols for the scanned-source data represent positions where the measurements are not as reliable because of a smaller signal-to-noise ratio.)

should be valid even in the critical regime. The parameter A quantifies the magnitude of C_2 and C_3 correlations, $C_0^{(\mathrm{in})}$ characterizes the magnitude of the genuine C_0 correlation due to the LDOS fluctuations at the source point, and $C_0^{(\mathrm{out})}$ measures the amplitude of the short-range contribution to C_0 due to scattering in the vicinity of both detectors when the latter are close to each other [35]. $C_0^{(\mathrm{in})}$ is the asymptotic value of $C_\omega(\Delta r)$ for $\Delta r \to \infty$. The solid lines in Fig. 1 show the results of performing a *joint* weighted fit of these theoretical predictions to both the single- and scanned-source data, thereby determining the values of the parameters shown in Table I. In this fit, we account for the fact that $C_0^{(\mathrm{in})}$ contributes only to the scanned-source correlations and set $C_0^{(\mathrm{in})} = 0$ for fitting the single-source data; also, since the detector geometry is the same for both experiments, $C_0^{(\mathrm{out})}$ is constrained to have a common value for the two curves. Note that for white-noise uncorrelated disorder and a pointlike source and detector in an infinite disordered medium, $C_0^{(\mathrm{in})} = C_0^{(\mathrm{out})} = \pi/k\ell$ [22]. In our experiments, however, both the source and detector have finite extent (which differs in each case [35]), and the finite size of the aluminum beads inevitably results in some short-range structural correlations. Therefore, we expect, in general, that $C_0^{(\mathrm{in})} \neq C_0^{(\mathrm{out})} \neq \pi/k\ell$ [23]. Figure 1 provides strong evidence that the large asymptotic value of $C_\omega(\Delta r \to \infty) = C_0^{(\mathrm{in})} \sim 1$ for the scanned-source experiment is due to C_0 correlations.

Similar behavior, with $C_0^{(\mathrm{in})} \sim 1$, is observed over a broad frequency range from 1.6 to 2.8 MHz, where independent

TABLE I. Fit parameters, with uncertainties in parentheses. The uncertainties are given by the standard deviation of the parameters. For a point source and detector, the normalized variance, $C(0,0)$, depends on all three parameters: $C(0,0) = 1 + 2[A + C_0^{(\mathrm{in})} + C_0^{(\mathrm{out})}]$. By contrast, the infinite-range contributions depend independently on the different contributions to C_0, with the asymptotic values of the scanned-source $C(\Delta r, 0)$, the single-source $C(0,\Omega)$, and the scanned-source $C(0,\Omega)$ being equal to $C_0^{(\mathrm{in})}$, $C_0^{(\mathrm{out})}$, and $C_0^{(\mathrm{in})} + C_0^{(\mathrm{out})}$, respectively.

Parameter	2.4 MHz	0.97 MHz	1.07 MHz	1.11 MHz
Spatial correlations				
A (single)	0.50 (0.02)	0.48 (0.02)	1.29 (0.04)	1.59 (0.06)
A (scanned)	2 (1)	0.8 (0.2)	6 (1)	6 (3)
$C_0^{(\mathrm{in})}$	1.3 (0.2)	0.42 (0.02)	1.06 (0.08)	7.8 (0.5)
$C_0^{(\mathrm{out})}$	0.4 (0.2)	0.8 (0.2)	1.5 (0.4)	7 (1)
Frequency correlations				
A (single)		0.2 (0.2)	0.8 (0.3)	
A (scanned)		0.7 (0.1)	5.2 (0.8)	
$C_0^{(\mathrm{in})}$		0.32 (0.03)	0.9 (0.3)	
$C_0^{(\mathrm{out})}$		0.62 (0.06)	1.3 (0.1)	
$\Omega_{\mathrm{Th}}/2\pi$(kHz)		4.35 (0.09)	7.2 (0.1)	

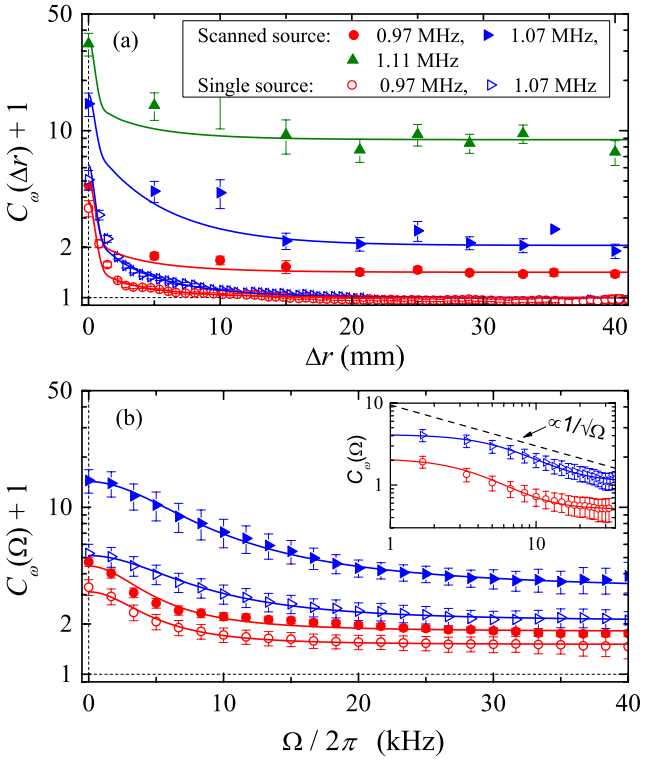

FIG. 2 (color online). Spatial (a) and frequency (b) correlations measured near 1 MHz, showing the increase of long-range correlations near a mobility edge. The inset shows the characteristic $1/\sqrt{\Omega}$ behavior expected for C_2 and C_3 correlations. For both plots, data have been averaged over a bandwidth of 25 kHz, except at the highest frequency (1.11 MHz), where the data are changing too rapidly with frequency to be meaningfully averaged. These rapid variations with frequency near 1.11 MHz also complicate measurements of frequency correlations, which are therefore not shown here. The error bars are calculated as in Fig. 1. Lines show the fits using the parameters given in Table I.

measurements of the dynamic transverse confinement of the transmitted intensity [10] indicate that ultrasound is still localized, with similar values of the localization length ξ ($\xi \approx L = 14.5$ mm for this sample in this frequency range). At lower frequencies, at least one ME must exist, since previous measurements on these samples revealed diffusive behavior at the much lower frequency of 200 kHz [10]. To investigate the long-range correlations as a ME is approached, experiments were performed at intermediate frequencies, between these well-established diffusive and localized regimes [10], with representative data near 1 MHz being presented in Fig. 2. Both spatial and frequency correlations increase significantly with frequency when a ME, which we estimate to be at approximately 1.1 MHz, is approached. In particular, the asymptotic value of the scanned-source spatial correlations, $C_0^{(\mathrm{in})}$, increases from 0.4 to almost 8 over the range of frequencies illustrated in Fig. 2(a).

The frequency correlations also show large increases in C_0 over this frequency range [see Fig. 2(b)] [36]. $C_\omega(\Omega)$ contains infinite-range contributions from scattering both near the source and near the detector; i.e., both $C_0^{(\mathrm{in})}$ and $C_0^{(\mathrm{out})}$ contribute to the asymptotic value of $C_\omega(\Omega)$ for large Ω [35]. The single-source measurements [which suppress $C_0^{(\mathrm{in})}$] show that $C_0^{(\mathrm{out})}$ increases from 0.6 to 1.3 between 0.97 and 1.07 MHz. By comparing the best-fit values (see Table I), we see that for the scanned-source case, $C_0^{(\mathrm{in})}$ and $C_0^{(\mathrm{out})}$ are of the same order of magnitude, as could be expected from the roughly symmetric arrangement of the experiment [37].

The C_2 and C_3 correlations, quantified by parameter A, also increase with frequency around 1 MHz, as found from the data for both spatial and frequency correlations (see Fig. 2 and Table I). Because $A \propto 1/(k\ell^*)^2$ to leading order [35], where ℓ^* is the transport mean free path, the increase of A corresponds to a decrease of $k\ell^*$ as the ME is approached. In addition, the values of A found from the fits are always larger in the scanned-source case. Keeping the source fixed not only suppresses $C_0^{(\mathrm{in})}$ but also reduces the magnitude of long-range C_2 and C_3 correlations because the latter correlations contain contributions from scattering in the vicinity of the source. This effect does not preclude the clear identification of C_0 that stands out by its infinite range in both space and frequency.

The frequency dependence of the asymptotic value of the spatial intensity correlation function between 0.6 and 1.4 MHz is shown in Fig. 3(a). These data are the average of the measured correlations for Δr between 25 and 50 mm, where $C_\omega(\Delta r)$ is found to be independent of distance, providing accurate measurements of $C_\omega(\Delta r \to \infty) = C_0^{(\mathrm{in})}$ when the source is scanned. It increases rapidly with frequency near 0.78 and 1.11 MHz, reaching values up to 13 here, and even as high as 30 in other experiments—by

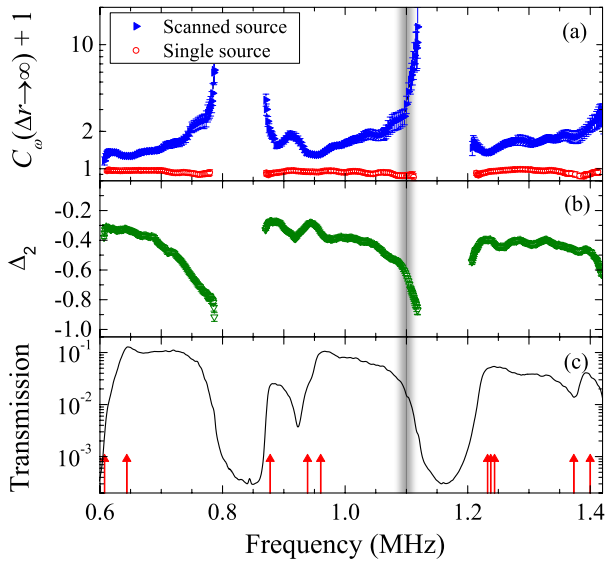

FIG. 3 (color online). (a) Frequency dependence of the asymptotic value of the spatial correlation $C_\omega(\Delta r \to \infty) = C_0^{(\mathrm{in})}$ for single and scanned point sources, (b) anomalous dimension Δ_2 of the generalized inverse participation ratio for $q = 2$, and (c) the amplitude transmission coefficient. The arrows in (c) indicate the resonant frequencies of individual aluminum beads. $C_0^{(\mathrm{in})}$ and Δ_2 show large increases in magnitude near the upper band edges, where we expect mobility edges to occur. The grey vertical line indicates the location of the ME near 1.1 MHz, estimated from transverse confinement measurements.

far the largest values of C_0 ever reported. A comparison of these results with the amplitude transmission coefficient [Fig. 3(c)] reveals that the frequencies where C_0 increases rapidly coincide with the upper edges of pass bands in these disordered structures. In the band gaps, the transmission becomes too small for long-range correlations to be measured. As explained in Refs. [10,38], these band gaps are not due to Bragg scattering, as in phononic crystals [39]. Instead, they arise between pass bands formed from coupled resonances of the beads when the coupling is sufficiently weak.

Near the upper edges of the pass bands, where the average density of states decreases, mobility edges between extended and localized states may be expected [40]. Evidence that mobility edges do indeed occur near these band edges has been obtained through separate measurements of increased spatial confinement of the transmitted intensity near the upper band edges relative to the pass band centers, using the method developed by Hu *et al.* [10]. This evidence is most compelling for the ME near 1.1 MHz, which is indicated by the vertical line in Fig. 3. Additional evidence can be inferred from the large increases that are found in the normalized intensity variance, $C_\omega(\Delta r = 0, \Omega = 0)$, near the upper band edges (e.g., Fig. 2 and Ref. [10]). Thus, the large increases in C_0 near 0.78 and 1.1 MHz must be due to large LDOS fluctuations near Anderson transitions in these samples, suggesting that C_0 is sensitive to critical effects.

This interpretation of the striking increase in C_0 near the band edges is further supported by measurements of the anomalous multifractal dimension Δ_2, which characterizes the length-scale dependence of the inverse participation ratio (IPR) $P_2 \sim L^{-d-\Delta_2}$ [41]. The significant decrease in Δ_2 near the upper band edges [Fig. 3(b)] is consistent with the expected behavior near the Anderson transition, where Δ_2 should become increasingly negative, varying from 0 in the diffuse regime to -2 deep in localized regime [4]. Since the source and detector in our experiments are pointlike, it is likely that a single mode dominates at any frequency, so we expect the IPR calculated from the intensity $I(\mathbf{r})$ and from the LDOS $\rho(\mathbf{r})$ to be equal [28,33]. Then, $P_2 = L^{-d}\langle\rho^2\rangle/\langle\rho\rangle^2 = L^{-d}[C_0(\infty)+1]$, and we predict that $\log\,[C_0(\infty)+1] \propto -\Delta_2$. Within experimental error, the frequency dependencies of $C_\omega(\Delta r \to \infty) = C_0^{(\mathrm{in})}$ and Δ_2 [Figs. 3(a) and (b)] are consistent with this prediction. Thus, not only do the infinite-range correlations and the IPR show evidence of transitions from extended to localized behavior near the upper band edges, but the correspondence between these measurements verifies the link between C_0, Δ_2, and LDOS fluctuations experimentally.

In conclusion, infinite-range intensity correlations have been measured directly in a strongly scattering 3D "mesoglass" for which Anderson localization of ultrasound was previously demonstrated [10]. Measurements are consistent with diagrammatic theory when large magnitudes of both long-range (C_2 and C_3) and infinite-range (C_0) terms are assumed. By varying the ultrasonic frequency, we have been able to investigate the growth not only of C_2 and C_3 but also of C_0 near the Anderson transition. Infinite-range correlations of order unity are found over a broad range of frequencies, reflecting the high LDOS contrast that can be achieved in our samples. The magnitude of these C_0 correlations is seen to increase dramatically as a ME is approached and crossed. These C_0 results are mirrored by the frequency dependence of the anomalous dimension Δ_2, which characterizes the size scaling of the inverse participation ratio. Our independent measurements of these two quantities establish a link between C_0 and Δ_2, revealing that C_0 can be used to probe the Anderson transition. The possibility of exploiting our findings to experimentally investigate critical behavior at the Anderson transition, by focusing on the possible one-parameter scaling of C_0 near the ME, is a promising new avenue for future research.

This work was supported by NSERC and by a PICS program of CNRS.

*John.Page@umanitoba.ca

[1] P. W. Anderson, Phys. Rev. **109**, 1492 (1958).
[2] E. Abrahams, P. W. Anderson, D. C. Licciardello, and T. V. Ramakrishnan, Phys. Rev. Lett. **42**, 673 (1979).
[3] D. Vollhardt and P. Wölfle, Phys. Rev. Lett. **45**, 842 (1980).

[4] F. Evers and A. D. Mirlin, Rev. Mod. Phys. **80**, 1355 (2008).
[5] P. Sheng, *Introduction to Wave Scattering, Localization and Mesoscopic Phenomena* (Springer, Berlin, 2006).
[6] *50 Years of Anderson Localization*, edited by E. Abrahams (World Scientific, Singapore, 2010).
[7] S. John, H. Sompolinsky, and M. J. Stephen, Phys. Rev. B **27**, 5592 (1983).
[8] S. John, Phys. Rev. Lett. **53**, 2169 (1984).
[9] P. W. Anderson, Philos. Mag. B **52**, 505 (1985).
[10] H. Hu, A. Strybulevych, J. H. Page, S. E. Skipetrov, and B. A. van Tiggelen, Nat. Phys. **4**, 945 (2008).
[11] T. Sperling, W. Bührer, C. M. Aegerter, and G. Maret, Nat. Photonics **7**, 48 (2013).
[12] S. Feng, C. Kane, P. A. Lee, and A. D. Stone, Phys. Rev. Lett. **61**, 834 (1988).
[13] J. F. de Boer, M. P. van Albada, and A. Lagendijk, Phys. Rev. B **45**, 658 (1992).
[14] R. Berkovits and S. Feng, Phys. Rep. **238**, 135 (1994).
[15] F. Scheffold, W. Härtl, G. Maret, and E. Matijević, Phys. Rev. B **56**, 10942 (1997).
[16] M. C. W. van Rossum and T. M. Nieuwenhuizen, Rev. Mod. Phys. **71**, 313 (1999).
[17] P. Sebbah, R. Pnini, and A. Z. Genack, Phys. Rev. E **62**, 7348 (2000).
[18] A. A. Chabanov, N. P. Trégourès, B. A. van Tiggelen, and A. Z. Genack, Phys. Rev. Lett. **92**, 173901 (2004).
[19] E. Akkermans and G. Montambaux, *Mesoscopic Physics of Electrons and Photons* (Cambridge University Press, Cambridge, 2007).
[20] A. Z. Genack, P. Sebbah, M. Stoytchev, and B. A. van Tiggelen, Phys. Rev. Lett. **82**, 715 (1999).
[21] M. L. Cowan, D. Anache-Ménier, W. K. Hildebrand, J. H. Page, and B. A. van Tiggelen, Phys. Rev. Lett. **99**, 094301 (2007).
[22] B. Shapiro, Phys. Rev. Lett. **83**, 4733 (1999).
[23] S. E. Skipetrov and R. Maynard, Phys. Rev. B **62**, 886 (2000).
[24] B. A. van Tiggelen and S. E. Skipetrov, Phys. Rev. E **73**, 045601 (2006).
[25] A. Cazé, R. Pierrat, and R. Carminati, Phys. Rev. A **82**, 043823 (2010).
[26] R. G. S. El-Dardiry, S. Faez, and A. Lagendijk, Phys. Rev. A **83**, 031801 (2011).
[27] M. D. Birowosuto, S. E. Skipetrov, W. L. Vos, and A. P. Mosk, Phys. Rev. Lett. **105**, 013904 (2010).
[28] V. Krachmalnicoff, E. Castanié, Y. De Wilde, and R. Carminati, Phys. Rev. Lett. **105**, 183901 (2010).
[29] R. Sapienza, P. Bondareff, R. Pierrat, B. Habert, R. Carminati, and N. F. van Hulst, Phys. Rev. Lett. **106**, 163902 (2011).
[30] P. D. García, S. Stobbe, I. Söllner, and P. Lodahl, Phys. Rev. Lett. **109**, 253902 (2012).
[31] A. D. Mirlin, Phys. Rep. **326**, 259 (2000).
[32] V. Dobrosavljević, A. A. Pastor, and B. K. Nikolić, Europhys. Lett. **62**, 76 (2003).
[33] N. C. Murphy, R. Wortis, and W. A. Atkinson, Phys. Rev. B **83**, 184206 (2011).
[34] The possible existence of a small infinite-range contribution to the intensity correlations was pointed out in Ref. [18] for waves in quasi-one-dimensional disordered waveguides, but their origin was not identified with certainty.
[35] See Supplemental Material at http://link.aps.org/supplemental/10.1103/PhysRevLett.112.073902 for the details of the experimental methods and theoretical analysis.
[36] The fits of the frequency correlations are performed similarly to those of the spatial correlations, with the additional parameter Ω_{Th} also constrained to have the same value for both single- and scanned-source experiments.
[37] Note that when both spatial and frequency correlations are measured, the values of both $C_0^{(\mathrm{in})}$ and $C_0^{(\mathrm{out})}$ can be determined most robustly from the asymptotic values of the correlations. For example, the fitted values of $C_0^{(\mathrm{out})}$ measured from the frequency correlations, which contain an infinite-range contribution due to $C_0^{(\mathrm{out})}$, are more reliable than those measured from the spatial correlations.
[38] J. A. Turner, M. E. Chambers, and R. L. Weaver, Acustica **84**, 628 (1998).
[39] S. Yang, J. H. Page, Z. Liu, M. L. Cowan, C. T. Chan, and P. Sheng, Phys. Rev. Lett. **88**, 104301 (2002).
[40] S. John, Phys. Rev. Lett. **58**, 2486 (1987).
[41] S. Faez, A. Strybulevych, J. H. Page, A. Lagendijk, and B. A. van Tiggelen, Phys. Rev. Lett. **103**, 155703 (2009).